Journal of Sound and Vibration (2002) **250**(2), 215–227
doi:10.1006/jsvi.2001.3919, available online at http://www.idealibrary.com on IDEAL®

DISPERSION OF WAVES IN IMMERSED LAMINATED COMPOSITE HOLLOW CYLINDERS

Z. C. Xi, G. R. Liu, K. Y. Lam and H. M. Shang

Department of Mechanical and Production Engineering, National University of Singapore, 10 Kent Ridge Crescent, Singapore 119260, *Singapore. E-mail: mpeliugr@nus.edu.sg*

(*Received* 7 *August* 2000, *and in final form* 20 *March* 2001)

A layer element method (LEM) is presented for analyzing frequency and group velocity dispersive behaviours of waves in a laminated composite cylinder surrounded by a fluid. The LEM applies finite elements to model the radial displacement of the cylinder and the radial pressure of the fluid, and complex exponentials to express the axial and circumferential displacements of the cylinder as well as the axial and tangential pressures of the fluid. The dispersive equation for the fluid-loaded cylinder follows from variational techniques. The frequency and group velocity dispersive relationships of the fluid-coupling cylinder are obtained by means of the Rayleigh quotient. Numerical results are given for hybrid laminated composite cylinders and cylindrical shells submerged in water. The addition of the fluid is proven to have considerable impact on the group velocity spectra of waves in laminated composite cylinders.

1. INTRODUCTION

Wave propagation in anisotropic media has been a subject of intense research interest in the last few decades. There now exists much work on Rayleigh, Lamb, Love and Stoneley waves in anisotropic media which were well reviewed [1–6].

As composite cylinders and cylindrical shells have been widely used in industrious fields of marine, petrochemical, nuclear and power generation, and so on, great effort has been directed towards study of waves propagating in anisotropic cylinders and cylindrical shells. Markus and Mead [7, 8], and Yuan and Hsieh [9] studied analytically free waves in composite cylindrical shells. Xi *et al.* [10–13] treated semi-analytically free waves of laminated composite shells of revolution either in vacuum or partially filled with a fluid. In their analyses, the effects of transverse shear deformation, material non-linearity, the coupling between symmetric and antisymmetric modes, and the coupling between the fluid and shell were taken into account. Han *et al.* [14] dealt with transient waves of cylindrical shells composed of functionally gradient materials. Rattanwangcharoen *et al.* [15] studied the reflection problem of waves at the free edge of composite cylinders. Rattanwangcharoen *et al.* [16] and Zhuang *et al.* [17] investigated axisymmetric guided waves scattered by cracks in welded steel pipes. Xi *et al.* [18–20] examined waves scattered by cracks in laminated composite cylinders either in vacuum or loaded by a fluid. Nelson *et al.* [21], and Huang and Dong [22] analyzed frequency spectra in laminated composite cylinders using analytical–numerical methods. Berliner and Solecki [23, 24] discussed analytically the frequency dispersive behaviours of waves in fluid-filled transversely isotropic cylinders. Xi *et al.* [25] investigated frequency spectra, group velocity spectra and characteristic surfaces of waves in laminated composite cylinders and

0022-460X/02/070215 + 13 $35.00/0

cylindrical shells using a semi-analytical procedure, but leave open the effect of fluid presence.

Laminated composite cylinders and cylindrical shells surrounded by a fluid are frequently encountered in practical engineering. Therefore, this paper intends to present a method for analyzing frequency and group velocity dispersive behaviours of waves in this type of fluid-loaded cylinder and cylindrical shell. In this approach, the radial displacement of the cylinder and the radial pressure of the fluid are modelled by finite elements, while the axial and circumferential displacements of the cylinder as well as the axial and tangential pressures of the fluid are expanded as the complex exponentials. The dispersive equation for the fluid-loaded cylinder follows from variational techniques. The frequency and group velocity dispersive relationships of the fluid-coupling system are established in terms of the Rayleigh quotient. The effects of the fluid addition, wave normal and propagation modes, ratio of radius to thickness and lay-ups on the frequency and group velocity spectra are discussed via numerical examples.

2. FORMULATION

Consider a laminated composite hollow cylinder of inner radius R_i and outer radius R_o, surrounded by an ideal fluid of outer radius R_f, as shown in Figure 1. The hollow cylinder has circular ends and straight slides. When the thickness of wall is large, we refer to it as a thick cylinder; when the thickness of wall is small, we refer to it as a cylindrical shell. Obviously, the wave propagation in the cylinder is of the helical form. Since the wave

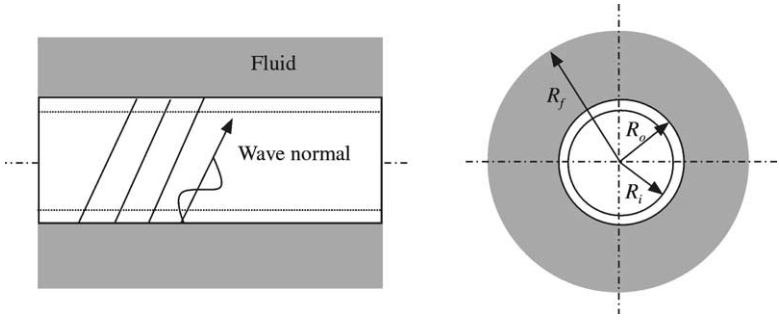

Figure 1. Laminated composite cylinder surrounded by fluid.

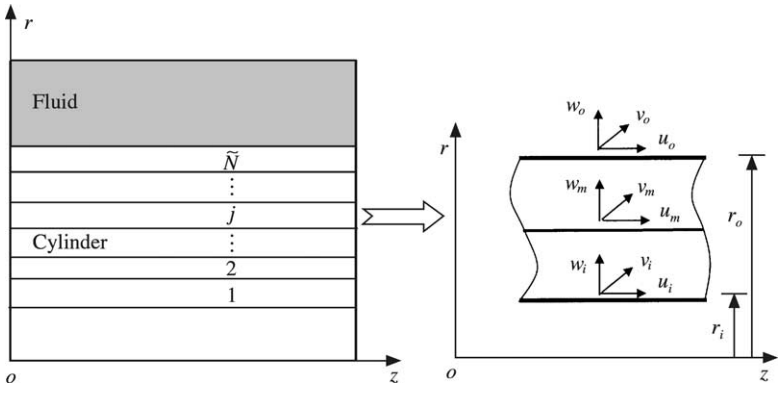

Figure 2. Annular solid element subdivision and the jth isolated element.

propagates in the in-surface of the cylinder only, we can handle the radial and in-surface displacements using the variable separation method. The in-surface helical wave may be conveniently expressed in the form of complex exponentials. In view of material heterogeneity associated with different materials and/or differing orientations in the various plies, it is suitable to use finite elements to model the radial variable of the wave. This treatment is similar to that by Nelson *et al.* [21].

In this study, an annular solid element shown in Figure 2 is used in the subdivision of the cylinder in the wall direction. The solid element has the inner, middle and outer nodal surfaces i, m, o, that have each three degrees of freedom, u, v, w. Hence, the vector of the unknown displacement amplitudes of the solid element is expressed as $\mathbf{U}^e = [u_i\ v_i\ w_i\ u_m\ v_m\ w_m\ u_o\ v_o\ w_o]^{\mathrm{T}}$, where the superscript e denotes the element. Suppose that the cylinder is subdivided into $\tilde{N}$ strip elements in the radial direction and the element numbering goes from the inner to outer surface, and that r_i and r_o represent, respectively, the inner and outer radii of any solid element j. The displacements $\mathbf{u} = [u\ v\ w]^{\mathrm{T}}$ within an element are thus approximated as

$$\mathbf{u} = \mathbf{N}(r)\mathbf{U}^e \exp \mathrm{i}(n\theta + k_z z - \omega t), \tag{1}$$

where n is the wave number in the circumferential direction and $k_z = k\cos\beta$ is the wave number in the axial direction. When the wave of wave number k propagates in the cylinder at an arbitrary β angle with respect to the z-axis, we have

$$n = R_o k \sin\beta, \qquad k_z = k\cos\beta. \tag{2}$$

In equation (1), $\mathbf{N}(r)$ is the shape function matrix of the solid element given by

$$\mathbf{N}(r) = \lfloor (1 - 3\hat{r} + 2\hat{r}^2)\mathbf{I} \quad 4(\hat{r} - \hat{r}^2)\mathbf{I} \quad (-\hat{r} + 2\hat{r}^2)\mathbf{I} \rfloor. \tag{3}$$

Here $\hat{r} = (r - r_i)/(r_o - r_i)$, $r_i \leqslant r \leqslant r_o$ and $\mathbf{I}$ is a 3×3 identity matrix. ω is the circular frequency.

With the displacement model, we can readily derive the dispersive equation for the cylinder by means of the Hamilton principle that takes the form

$$\int_{t_0}^{t_1} \delta(V - T)\,\mathrm{d}t = 0, \tag{4}$$

where t_0 and t_1 are time instants, and V and T are, respectively, the potential energy and kinetic energy of the solid element.

The kinetic energy of the solid element is expressed as

$$T = \frac{1}{2}\int_{-\infty}^{+\infty}\int_0^{2\pi}\int_{r_i}^{r_o} \frac{\partial \mathbf{u}^{\mathrm{T}}}{\partial t}\frac{\partial \mathbf{u}}{\partial t}\,\rho r\,\mathrm{d}r\,\mathrm{d}\theta\,\mathrm{d}z, \tag{5}$$

where ρ is the mass density of the material of the solid element.

The potential energy of the solid element in the absence of body forces is given by

$$V = \frac{1}{2}\int_{-\infty}^{+\infty}\int_0^{2\pi}\int_{r_i}^{r_o} \boldsymbol{\varepsilon}^{\mathrm{T}}\boldsymbol{\sigma} r\,\mathrm{d}r\,\mathrm{d}\theta\,\mathrm{d}z - \int_{-\infty}^{+\infty}\int_0^{2\pi} (\mathbf{u}_i^{\mathrm{T}}\mathbf{T}_i r_i + \mathbf{u}_o^{\mathrm{T}}\mathbf{T}_o r_o)\,\mathrm{d}\theta\,\mathrm{d}z, \tag{6}$$

where $\mathbf{u}_i$, $\mathbf{u}_o$ are, respectively, the vectors of the inner and outer surface displacements of the solid element, $\mathbf{T}_i$, $\mathbf{T}_o$ are, respectively, the tractions on the inner and outer surfaces of the solid element, $\boldsymbol{\varepsilon} = [\varepsilon_z\ \varepsilon_\theta\ \varepsilon_r\ \gamma_{r\theta}\ \gamma_{rz}\ \gamma_{z\theta}]^{\mathrm{T}}$ and $\boldsymbol{\sigma} = [\sigma_z\ \sigma_\theta\ \sigma_r\ \tau_{r\theta}\ \tau_{rz}\ \tau_{z\theta}]^{\mathrm{T}}$ are, respectively, the vectors of strains and stresses.

Under the assumption of small deformations, the strains are related to the displacements, in the cylindrical co-ordinate system by

$$\boldsymbol{\varepsilon} = \mathbf{L}\mathbf{u}, \tag{7}$$

where $\mathbf{L}$ is the differential operator matrix given by

$$\mathbf{L} = \begin{bmatrix} \dfrac{\partial}{\partial z} & 0 & 0 & 0 & \dfrac{\partial}{\partial r} & \dfrac{1}{r}\dfrac{\partial}{\partial \theta} \\ 0 & \dfrac{1}{r}\dfrac{\partial}{\partial \theta} & 0 & \dfrac{\partial}{\partial r} - \dfrac{1}{r} & 0 & \dfrac{\partial}{\partial z} \\ 0 & \dfrac{1}{r} & \dfrac{\partial}{\partial r} & \dfrac{1}{r}\dfrac{\partial}{\partial \theta} & \dfrac{\partial}{\partial z} & 0 \end{bmatrix}^{\mathrm{T}} = \mathbf{L}_1 \frac{\partial}{\partial z} + \mathbf{L}_2 \frac{1}{r}\frac{\partial}{\partial \theta} + \mathbf{L}_3 \frac{\partial}{\partial r} + \mathbf{L}_4 \frac{\mathbf{1}}{r}. \tag{8}$$

Here $\mathbf{L}_1$, $\mathbf{L}_2$, $\mathbf{L}_3$ and $\mathbf{L}_4$ can be obtained by inspection from equation (8).

Assume that the cylinder is composed of an arbitrary number of linearly elastic, shell-like, transversely isotropic plies and that the bonding between plies is perfect. Then, the off-principal-axis stress–strain relations for any ply are given by

$$\boldsymbol{\sigma} = \bar{\mathbf{Q}}\boldsymbol{\varepsilon}, \tag{9}$$

where $\bar{\mathbf{Q}}$ is the matrix of the off-principal-axis stiffness coefficients of the ply. The stiffness coefficient matrix is symmetric. Their expressions in terms of engineering constants are given by Vinson and Sierakowski [26].

Invoking equations (7)–(9), equation (6) may be rewritten as

$$\begin{aligned} V = \frac{1}{2}\int_{-\infty}^{+\infty}\int_0^{2\pi}\int_{r_i}^{r_o}\Bigg(& \frac{\partial \mathbf{u}^{\mathrm{T}}}{\partial z}\mathbf{D}_{11}\frac{\partial \mathbf{u}}{\partial z} + \frac{1}{r}\frac{\partial \mathbf{u}^{\mathrm{T}}}{\partial z}\mathbf{D}_{12}\frac{\partial \mathbf{u}}{\partial \theta} + \frac{\partial \mathbf{u}^{\mathrm{T}}}{\partial z}\mathbf{D}_{13}\frac{\partial \mathbf{u}}{\partial r} + \frac{1}{\gamma}\frac{\partial \mathbf{u}^{\mathrm{T}}}{\partial z}\mathbf{D}_{14}\mathbf{u} \\ & + \frac{1}{r}\frac{\partial \mathbf{u}^{\mathrm{T}}}{\partial \theta}\mathbf{D}_{12}^{\mathrm{T}}\frac{\partial \mathbf{u}}{\partial z} + \frac{1}{r^2}\frac{\partial \mathbf{u}^{\mathrm{T}}}{\partial \theta}\mathbf{D}_{22}\frac{\partial \mathbf{u}}{\partial \theta} + \frac{1}{r}\frac{\partial \mathbf{u}^{\mathrm{T}}}{\partial \theta}\mathbf{D}_{23}\frac{\partial \mathbf{u}}{\partial r} + \frac{1}{r^2}\frac{\partial \mathbf{u}^{\mathrm{T}}}{\partial \theta}\mathbf{D}_{24}\mathbf{u} \\ & + \frac{\partial \mathbf{u}^{\mathrm{T}}}{\partial r}\mathbf{D}_{13}^{\mathrm{T}}\frac{\partial \mathbf{u}}{\partial z} + \frac{1}{r}\frac{\partial \mathbf{u}^{\mathrm{T}}}{\partial r}\mathbf{D}_{23}^{\mathrm{T}}\frac{\partial \mathbf{u}}{\partial \theta} + \frac{\partial \mathbf{u}^{\mathrm{T}}}{\partial r}\mathbf{D}_{33}\frac{\partial \mathbf{u}}{\partial r} + \frac{1}{r}\frac{\partial \mathbf{u}^{\mathrm{T}}}{\partial r}\mathbf{D}_{34}\mathbf{u} \\ & + \frac{1}{r}\mathbf{u}^{\mathrm{T}}\mathbf{D}_{14}^{\mathrm{T}}\frac{\partial \mathbf{u}}{\partial z} + \frac{1}{r^2}\mathbf{u}^{\mathrm{T}}\mathbf{D}_{24}^{\mathrm{T}}\frac{\partial \mathbf{u}}{\partial \theta} + \frac{\mathbf{1}}{r}\mathbf{u}^{\mathrm{T}}\mathbf{D}_{34}^{\mathrm{T}}\frac{\partial \mathbf{u}}{\partial r} + \frac{1}{r^2}\mathbf{u}^{\mathrm{T}}\mathbf{D}_{44}\mathbf{u}\Bigg) r\,\mathrm{d}r\,\mathrm{d}\theta\,\mathrm{d}z \\ & - \int_{-\infty}^{+\infty}\int_0^{2\pi}(\mathbf{u}_i^{\mathrm{T}}\mathbf{T}_i r_i + \mathbf{u}_o^{\mathrm{T}}\mathbf{T}_o r_o)\,\mathrm{d}\theta\,\mathrm{d}z, \end{aligned} \tag{10}$$

where $\mathbf{D}_{ij} = \mathbf{L}_i^{\mathrm{T}}\bar{\mathbf{Q}}\mathbf{L}_j$ $(i, j = 1, 2, 3, 4)$.

Substituting equations (5) and (10) into equation (4), and carrying out variation with respect to $\mathbf{U}^e$, we find the dispersive equation for the solid element

$$(\mathbf{K}_c^e - \omega^2\mathbf{M}_c^e)\mathbf{U}^e - \mathbf{F}^e = 0, \tag{11}$$

where the subscript c denotes the cylinder,

$$\mathbf{K}_c^e = \mathbf{A}_1^e k_z^2 + \mathbf{A}_2^e n k_z + \mathbf{A}_3^e n^2 + \mathrm{i}\mathbf{A}_4^e k_z + \mathrm{i}\mathbf{A}_3^e n + \mathbf{A}_6^e, \tag{12}$$

$$\mathbf{M}_c^e = \int_{r_i}^{r_o} \mathbf{N}^{\mathrm{T}} \mathbf{N} \rho r \, \mathrm{d}r \tag{13}$$

and

$$\mathbf{F}^e = \mathbf{N}^{\mathrm{T}}|_{r=r_i} \mathbf{T}_i r_i + \mathbf{N}^{\mathrm{T}}|_{r=r_o} \mathbf{T}_o r_o \tag{14}$$

are the stiffness, mass and load matrices of the solid element respectively. $\mathbf{A}_i^e (i = 1, 2, \ldots, 6)$ in equation (12) are defined as

$$\mathbf{A}_1^e = \int_{r_i}^{r_o} \mathbf{N}^{\mathrm{T}} \mathbf{D}_{11} \mathbf{N} r \, \mathrm{d}r, \tag{15}$$

$$\mathbf{A}_2^e = \int_{r_i}^{r_o} \mathbf{N}^{\mathrm{T}} (\mathbf{D}_{12} + \mathbf{D}_{12}^{\mathrm{T}}) \mathbf{N} \, \mathrm{d}r, \tag{16}$$

$$\mathbf{A}_3^e = \int_{r_i}^{r_o} \frac{1}{r} \mathbf{N}^{\mathrm{T}} \mathbf{D}_{22} \mathbf{N} \, \mathrm{d}r, \tag{17}$$

$$\mathbf{A}_4^e = \int_{r_i}^{r_o} \left[-\mathbf{N}^{\mathrm{T}} \mathbf{D}_{13} \frac{\mathrm{d}\mathbf{N}}{\mathrm{d}r} + \frac{\mathrm{d}\mathbf{N}^{\mathrm{T}}}{\mathrm{d}r} \mathbf{D}_{13}^{\mathrm{T}} \mathbf{N} + \frac{1}{r} \mathbf{N}^{\mathrm{T}} (\mathbf{D}_{14}^{\mathrm{T}} - \mathbf{D}_{14}) \mathbf{N} \right] r \, \mathrm{d}r, \tag{18}$$

$$\mathbf{A}_5^e = \int_{r_i}^{r_o} \left[-\mathbf{N}^{\mathrm{T}} \mathbf{D}_{23} \frac{\mathrm{d}\mathbf{N}}{\mathrm{d}r} + \frac{\mathrm{d}\mathbf{N}^{\mathrm{T}}}{\mathrm{d}r} \mathbf{D}_{23}^{\mathrm{T}} \mathbf{N} + \frac{1}{r} \mathbf{N}^{\mathrm{T}} (\mathbf{D}_{24}^{\mathrm{T}} - \mathbf{D}_{24}) \mathbf{N} \right] r \, \mathrm{d}r, \tag{19}$$

$$\mathbf{A}_6^e = \int_{r_i}^{r_o} \left(\frac{\mathrm{d}\mathbf{N}^{\mathrm{T}}}{\mathrm{d}r} \mathbf{D}_{33} \frac{\mathrm{d}\mathbf{N}}{\mathrm{d}r} + \frac{1}{r} \frac{\mathrm{d}\mathbf{N}^{\mathrm{T}}}{\mathrm{d}r} \mathbf{D}_{34} \mathbf{N} + \frac{1}{r} \mathbf{N}^{\mathrm{T}} \mathbf{D}_{34}^{\mathrm{T}} \frac{\mathrm{d}\mathbf{N}}{\mathrm{d}r} + \frac{1}{r^2} \mathbf{N}^{\mathrm{T}} \mathbf{D}_{44} \mathbf{N} \right) r \, \mathrm{d}r. \tag{20}$$

The dispersive equation for the cylinder can be obtained through assembling all of the elements at the nodal surfaces. The boundary conditions on the cylinder–fluid interface and the inner surface of the cylinder as well as the interface conditions between the solid elements are

$$\mathbf{T}_1^i = 0, \tag{21}$$

$$\mathbf{T}_j^o = \mathbf{T}_{j+1}^i, \quad \mathbf{U}_j^o = \mathbf{U}_{j+1}^i \quad \text{for } 1 < j < \tilde{N} - 1, \tag{22}$$

$$\mathbf{T}_N^o = [0 \; 0 \; p]^{\mathrm{T}} = \mathbf{n}^{\mathrm{T}} p, \tag{23}$$

where p is the hydrodynamic pressure acting on the outer surface of the cylinder that is expressed as $p = \mathbf{N}_f|_{r=R_o} \mathbf{P}$ from below, the subscripts denote the element numbers, and the superscripts denote the inner and outer nodal surfaces of the solid element.

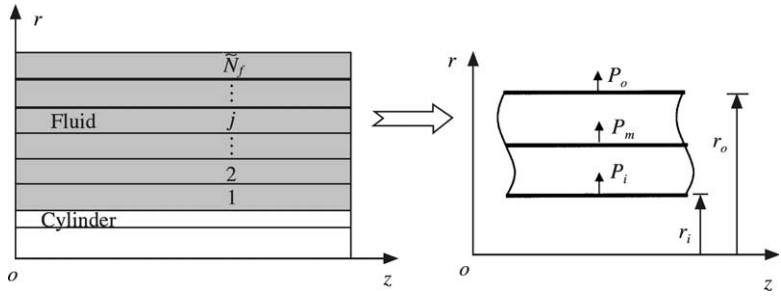

Figure 3. Annular fluid element subdivision and the *j*th isolated element.

Using equations (21)–(23) to assemble elements at the nodal surfaces, we get the dispersive equation for the cylinder

$$(\mathbf{K}_c - \omega^2 \mathbf{M}_c)\mathbf{U} - \mathbf{F}\mathbf{P} = 0, \tag{24}$$

where

$$\mathbf{F} = R_o \mathbf{N}^{\mathrm{T}}|_{r=R_o} \mathbf{n}^{\mathrm{T}} \mathbf{N}_f|_{r=R_o} \tag{25}$$

is referred to as the coupling matrix, through which the hydrodynamic pressure of the fluid affects the displacements of the cylinder.

We can analyze the fluid in a similar way. The pressure variation in the radial direction is modelled by annular fluid elements, while the pressure variations in the axial and circumferential directions are expanded as complex exponentials. The annular fluid element used is shown in Figure 3. The fluid element has the inner, middle and outer nodal surfaces, *i*, *m*, *o*, and each nodal surface has one degree of freedom, *p*. Hence, the vector of nodal-surface unknown pressure amplitudes of the fluid element is expressed as $\mathbf{P}^e(\theta, z, t) = [p_i\, p_m\, p_o]^{\mathrm{T}}$. Suppose that the fluid is subdivided into $\tilde{N}_f$ fluid elements in the radial direction and element numbering goes from the inner to outer surface, and that r_i and r_o represent, respectively, the inner and outer radii of any fluid element *j*. Thus, the hydrodynamic pressure within the fluid element may be expressed in terms of nodal-surface unknown pressure amplitudes as follows:

$$p(r, \theta, z, t) = \mathbf{N}_f(r)\mathbf{P}^e \exp \mathrm{i}(n\theta + k_z z - \omega t), \tag{26}$$

where

$$\mathbf{N}_f(r) = [(1 - 3\hat{r} + 2\hat{r}^2) \quad 4(\hat{r} - \hat{r}^2) \quad (-\hat{r} + 2\hat{r}^2)] \tag{27}$$

is the shape function matrix of the fluid element.

The dispersive equation for the fluid element can be derived by way of variational technique. From the fluid dynamic equilibrium and continuity equations, we obtain the following dynamic equilibrium in terms of the hydrodynamic pressure:

$$\frac{\partial^2 p}{\partial r^2} + \frac{1}{r}\frac{\partial p}{\partial r} + \frac{1}{r^2}\frac{\partial^2 p}{\partial \theta^2} + \frac{\partial^2 p}{\partial z^2} - \frac{1}{c^2}\frac{\partial^2 p}{\partial t^2} = 0, \tag{28}$$

where c is the speed of sound in the fluid and t is the time. To use variational technique, we need to construct a functional for the fluid element that is equivalent to equation (28). By means of variational method, we can readily develop the functional

$$\Pi = \frac{1}{2}\int_{-\infty}^{+\infty}\int_{0}^{2\pi}\int_{r_i}^{r_o}\left(\frac{\partial p}{\partial r}\frac{\partial p}{\partial r}+\frac{1}{r^2}\frac{\partial p}{\partial \theta}\frac{\partial p}{\partial \theta}+\frac{\partial p}{\partial z}\frac{\partial p}{\partial z}+\frac{2p}{c^2}\frac{\partial^2 p}{\partial t^2}\right)r\,\mathrm{d}r\,\mathrm{d}\theta\,\mathrm{d}z$$
$$-\int_{-\infty}^{+\infty}\int_{0}^{2\pi}\left(\frac{\partial p_i}{\partial r}p_i r_i+\frac{\partial p_o}{\partial r}p_o r_o\right)\mathrm{d}\theta\,\mathrm{d}z, \tag{29}$$

where the volume integration represents the energy due to the hydrodynamic pressure; the area integration represents the potential energy due to the pressures on the nodal surfaces of the fluid element. Substituting equation (26) into equation (29) and performing variational manipulation of Π with respect to $\mathbf{P}^e$ leads to the dispersive equation for the fluid element

$$(\mathbf{K}_f^e - \omega^2\mathbf{M}_f^e)\mathbf{P}^e - \mathbf{F}_f^e = 0, \tag{30}$$

where

$$\mathbf{K}_f^e = \mathbf{A}_{f1}^e k_z^2 + \mathbf{A}_{f2}^e \mathbf{n}^2 + \mathbf{A}_{f3}^e, \tag{31}$$

$$\mathbf{M}_f^e = \int_{r_i}^{r_o}\frac{1}{c^2}\mathbf{N}_f^{\mathrm{T}}\mathbf{N}_f r\,\mathrm{d}r \tag{32}$$

and

$$\mathbf{F}_f^e = \left(\mathbf{N}_f^{\mathrm{T}}|_{r=r_i}\frac{\partial p_i}{\partial r}r_i + \mathbf{N}_f^{\mathrm{T}}|_{r=r_o}\frac{\partial p_o}{\partial r}r_o\right) \tag{33}$$

are the stiffness, mass and load matrices of the fluid element respectively. $\mathbf{A}_{fi}^e (i = 1, 2, 3)$ in equation (31) are defined as

$$\mathbf{A}_{f1}^e = \int_{r_i}^{r_o}\mathbf{N}_f^{\mathrm{T}}\mathbf{N}_f r\,\mathrm{d}r, \tag{34}$$

$$\mathbf{A}_{f2}^e = \int_{r_i}^{r_o}\frac{1}{r}\mathbf{N}_f^{\mathrm{T}}\mathbf{N}_f\,\mathrm{d}r, \tag{35}$$

$$\mathbf{A}_{f3}^e = \int_{r_i}^{r_o}\frac{\mathrm{d}\mathbf{N}_f^{\mathrm{T}}}{\mathrm{d}r}\frac{\mathrm{d}\mathbf{N}_f}{\mathrm{d}r}r\,\mathrm{d}r. \tag{36}$$

The dispersive equation for the fluid can be obtained by assembling all of the fluid elements at the nodal surfaces. Since the fluid–cylinder coupling effect occurs only in the vicinity of the interface between the fluid and cylinder, for $R_f \to \infty$, the hydrodynamic pressure along the outer surface of the fluid vanishes. The boundary conditions on the interface between the fluid and cylinder, and the interface conditions between the fluid elements are

$$\left(\frac{\partial p}{\partial r}\right)_1^i = -\rho_f\frac{\partial^2 \bar{w}}{\partial t^2}, \tag{37}$$

$$p_j^o = p_{j+1}^i, \quad \left(\frac{\partial p}{\partial r}\right)_j^o = \left(\frac{\partial p}{\partial r}\right)_{j+1}^i \quad \text{for } 1 < j < \tilde{N}_f - 1, \tag{38}$$

where the subscripts denote the element numbers, the superscripts denote the inner and outer surfaces of the fluid element, and ρ_f is the density of the fluid. The quantity $\bar{w}$ is the radial displacement on the outer surface of the cylinder that is written as $\bar{w} = \mathbf{nNU}$ from the above.

Using equations (37) and (38) to assemble all of the elements at the nodal surfaces, we get the dispersive equation for the fluid

$$(\mathbf{K}_f - \omega^2 \mathbf{M}_f)\mathbf{P} - \rho_f \omega^2 \mathbf{F}^{\mathrm{T}} \mathbf{U} = 0, \tag{39}$$

where the coupling matrix $\mathbf{F}$ is the same as that given in equation (25).

Finally, the results of equations (24) and (39) can be combined as follows:

$$\left(\begin{bmatrix} \mathbf{K}_c & -\mathbf{F} \\ 0 & \mathbf{K}_f \end{bmatrix} - \omega^2 \begin{bmatrix} \mathbf{M}_c & 0 \\ \rho_f \mathbf{F}^{\mathrm{T}} & \mathbf{M}_f \end{bmatrix} \right) \begin{Bmatrix} \mathbf{U} \\ \mathbf{P} \end{Bmatrix} = \mathbf{0} \tag{40}$$

or in compact form

$$(\mathbf{K} - \omega^2 \mathbf{M})\varphi = \mathbf{0}. \tag{41}$$

This equation is referred to as the dispersive equation for the fluid-loaded cylinder. When the wave number k is specified, we can solve equation (41) for the circular frequency of the cylinder submerged in a fluid, and accordingly obtain the relationship between the wave number k and circular frequency ω; this relationship is called the dispersive relationship for the fluid-loaded cylinder.

With the aid of Rayleigh's quotient, we can conveniently express the circular frequency for the mth mode as

$$\omega_m^2 = \frac{\varphi_m^L \mathbf{K} \varphi_m^R}{\varphi_m^L \mathbf{M} \varphi_m^R}, \tag{42}$$

where φ_m^L and φ_m^R are the mth transposed left and right eigenvectors of equation (41).

The group velocity, at which energy is transported, is defined as

$$c_g = \mathrm{d}\omega/\mathrm{d}k. \tag{43}$$

Differentiation of equation (42) with respect to k provides the group velocity for the mth mode

$$c_{gm} = \frac{\varphi_m^L \mathbf{K}_{,k} \varphi_m^R}{2\omega_m \varphi_m^L \mathbf{M} \varphi_m^R}, \tag{44}$$

where

$$\mathbf{K}_{,k} = \begin{bmatrix} \dfrac{\partial K_c}{\partial k} & 0 \\ 0 & \dfrac{\partial K_f}{\partial k} \end{bmatrix}. \tag{45}$$

3. NUMERICAL RESULTS AND DISCUSSION

In what follows, numerical examples are employed to illustrate graphically the dispersive behaviours of a laminated composite cylinder surrounded by a fluid. In laminate codes used, a lamina numbering increases from the inner to outer surface; the letters C and G represent carbon/epoxy and glass/epoxy, respectively; the number following the letters indicates the fibre orientation with respect to the z-axis; the subscript s denotes that the laminated shell is symmetrically stacked about the middle surface. For the sake of simplicity, the following dimensionless parameters are adopted:

$$\bar{k} = k(R_o - R_i),\ \bar{\lambda} = \lambda/(R_o - R_i),\ \bar{R} = R_i/(R_o - R_i),$$

$$\bar{R}_f = R_f/R_o,\ \bar{\rho} = \rho_f/\rho,\ \bar{\omega} = \omega(R_o - R_i)\sqrt{\rho/Q_{11}},$$

where Q_{11} and ρ are the reference properties and taken as Young's modulus in the fibre direction and mass density of $C0$. The material properties of the cylinder are taken from Takahashi and Chou [27]. The fluid is taken as water of $\rho_f = 1{\cdot}0\,\mathrm{g/cm^3}$, $c = 1{\cdot}48 \times 10^3\,\mathrm{m/s}$ and $\bar{R}_f = 20$. Since the present method is within the framework of the theory of three-dimensional elasticity, it is applicable not only to a cylinder but also to a circular cylindrical shell. Thus, to discuss the distinction between them, two ratios of radius to thickness $\bar{R} = 1$ and 100 are used. In this study, a cylinder of $\bar{R} = 100$ is termed a cylindrical shell simply.

When the radius tends to be large, the results for the cylindrical shell approach those for the appropriate plate. To verify the present formulation and its numerical implementation, a validation of the numerical results against previously published data is provided for a $(C0/G \pm 45)_s$ plate. The value of the radius is $\bar{R} = 100$. It has been found that, as shown in Figure 4, the computed results compare very well with published results [28]. The results for the plate were obtained by Liu *et al.* using a hybrid-numerical method.

Next, we turn to the computation of the frequency spectra in a laminated composite cylinder and cylindrical shell surrounded by a fluid. The dispersion curves for an immersed $(C0/G \pm 45)_s$ cylindrical shell are illustrated in Figures 5(a) and 5(b), and compared with those for the corresponding cylindrical shell in vacuum. The propagation directions of

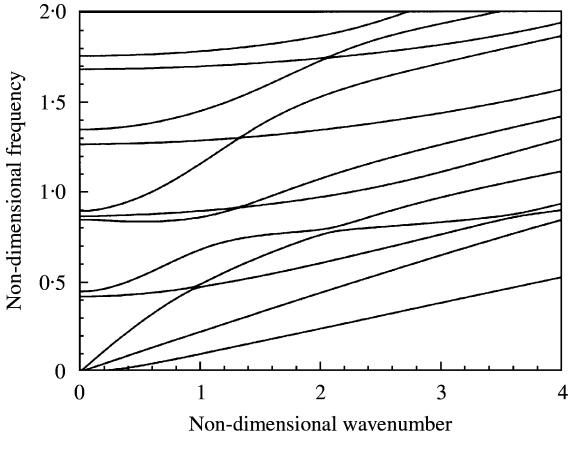

Figure 4. Dispersion curves for axial waves propagation in a $(C0/G \pm 45)_s$ plate: ——, present analysis; – – –, Liu *et al.* [28].

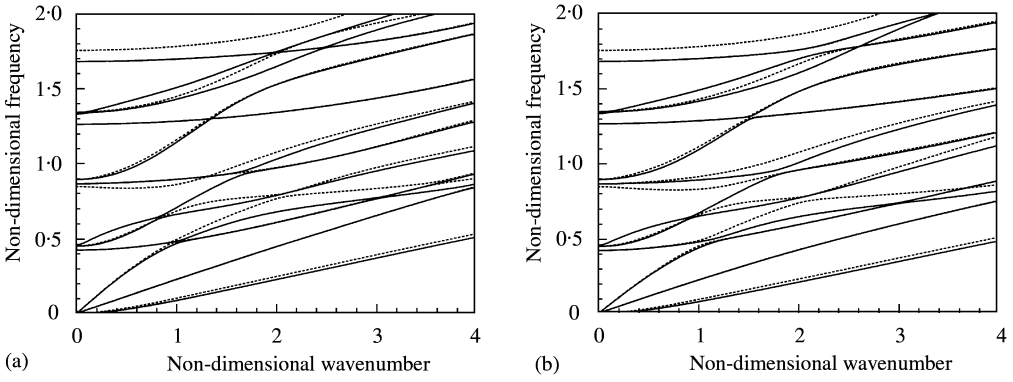

Figure 5. Dispersion curves for waves propagating in a $(C0/G \pm 45)_s$ cylindrical shell. (a) $\beta = 0$; (b) $\beta = 30°$. ——, wet shell; – – –, dry shell.

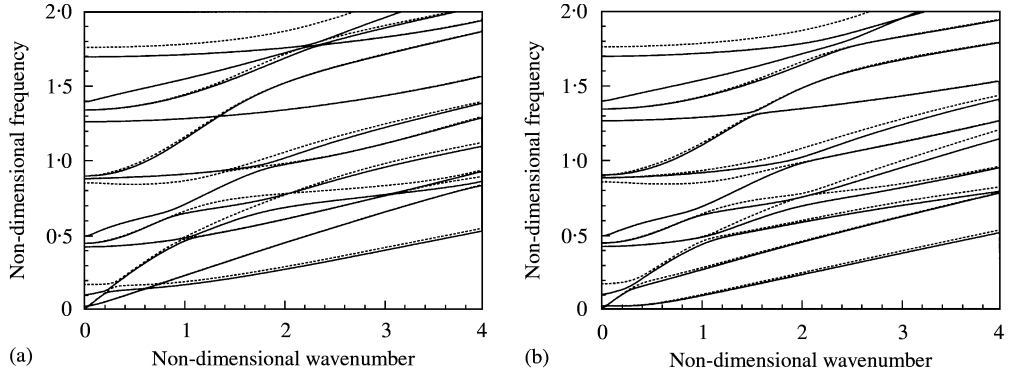

Figure 6. Dispersion curves for waves propagating in a $(C0/G \pm 45)_s$ cylinder. (a) $\beta = 0$; (b) $\beta = 30°$. ——, wet cylinder; – – –, dry cylinder.

waves are chosen as $\beta = 0$ and 30°, respectively; the former is for the axial wave; the latter is for the helical wave. Generally speaking, the presence of the fluid affects all of the frequencies to some extent. And this effect is dependent on the propagation mode and direction of waves. The interaction of the fluid and shell causes the reduction of the higher frequencies, but seems to have little impact on the lower frequencies. The fluid and shell coupling effect can be elaborated by way of the so-called added mass concept. The lower frequencies are dominated by the stiffness of the shell, while the higher frequencies are controlled by the mass of the shell. The addition of the fluid increases equivalently the mass of the shell and accordingly reduces the higher frequencies of the shell.

Figures 6(a) and 6(b) are the same as Figures 5(a) and 5(b) but for a cylinder. These results further confirm the preceding observations.

We now investigate the group velocity spectra in a laminated composite cylinder surrounded by a fluid. The group velocity spectra in an immersed $(C0/G \pm 45)_s$ cylindrical shell are illustrated in Figures 7(a) and 7(b), and compared with those for the corresponding dry case. The propagation directions of waves are also chosen as $\beta = 0$ and 30° respectively. From these two figures, it can be seen that the presence of the fluid causes the redistributions of the group velocity spectra in anisotropic shells. The difference between the amplitudes of the group velocity spectra is as apparent. The group velocities for most of

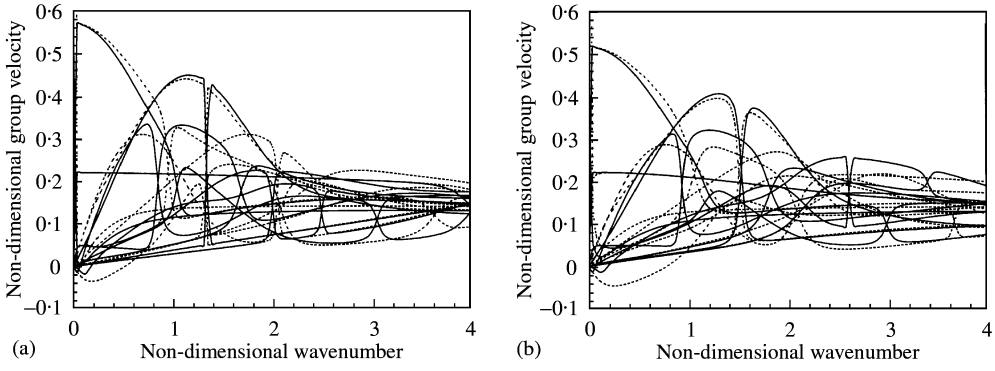

Figure 7. Group velocity spectra for waves propagating in a $(C0/G \pm 45)_s$ cylindrical shell. (a) $\beta = 0$; (b) $\beta = 30°$. ——, wet shell; – – –, dry shell.

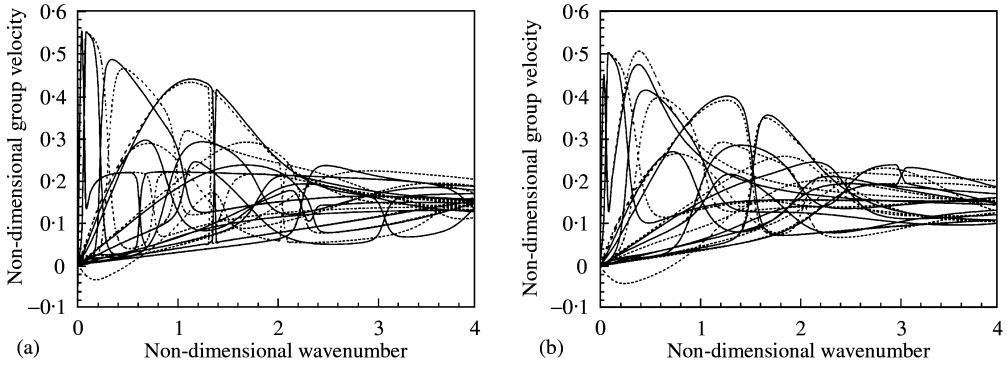

Figure 8. Group velocity spectra for waves propagating in a $(C0/G \pm 45)_s$ cylinder. (a) $\beta = 0$; (b) $\beta = 30°$. ——, wet cylinder; – – –, dry cylinder.

the propagation modes for the wet shell are smaller in magnitude than those for the appropriate dry shell. Only a few cases are otherwise. It is noteworthy that for a range of small wave numbers, the dry shell has negative group velocity, but the wet shell has not. Consequently, the presence of the fluid can prevent the phenomenon wherein energy propagates in the opposite direction to the wave normal. As mentioned above, the group velocity is one of the important concepts in wave propagation, as it is the rate at which energy is transported. The strong fluid–shell coupling effect implies that the dynamic design of an immersed composite cylindrical shell must account for the presence of the fluid.

Figures 8(a) and 8(b) are the same as Figures 7(a) and 7(b) but for a cylinder. The curves in these two figures once again demonstrate strong fluid–structural coupling effects.

4. CONCLUSIONS

An LEM has been presented for analyzing the dispersive behaviours and group velocity of waves in laminated composite cylinders surrounded by a fluid. The method of approach is formulated within the framework of the theory of three-dimensional elasticity, and is thus accurate in comparison with those using various approximate theories. The use of the LEM

not only is capable of reducing the spatial dimensions of a problem by one but also makes it easier to deal with cylinders composed of an arbitrary number of anisotropic layers, of arbitrary lay-ups and of any type of materials. Furthermore, the method is capable of omitting tedious pre-processors occupying a substantial part of finite element methods, and accordingly of reducing a great deal of computational labour. Numerical results indicate that the addition of the fluid has a strong influence on the group velocity of waves. Thus, the fluid–cylinder coupling effect must be taken into account in the dynamic design of immersed laminated composite cylinders and cylindrical shells.

REFERENCES

1. S. K. DATTA, H. M. LEDBETTER, Y. SHINDO and A. H. SHAH 1988 *Wave Motion* **10**, 171–182. Phase velocity and attenuation of plane elastic waves in a particle-reinforced composite medium.
2. S. K. DATTA, A. H. SHAH, R. L. BRATTON and T. CHAKRABORTY 1988 *Journal of Acoustical Society of America* **83**, 2020–2026. Wave propagation in laminated composite plates.
3. R. A. KLINE 1992 *Nondestructive Characterization of Composite Media*. Lancaster: Technomic.
4. A. H. NAYFEH 1995 *Wave Propagation in Layered Anisotropic Media with Applications to Composites*. Amsterdam: Elsevier.
5. J. L. ROSE 1999 *Ultrasonic Waves in Solid Media*. Cambridge: Cambridge University Press.
6. A. K. MAL 1988 *Wave Motion* **10**, 257–266. Wave propagation in layered composite laminates under periodic surface loads.
7. S. MARKUS and D. J. MEAD 1995 *Journal of Sound and Vibration* **181**, 127–147. Axisymmetric and asymmetric wave motion in orthotropic cylinders.
8. S. MARKUS and D. J. MEAD 1995 *Journal of Sound and Vibration* **181**, 149–167. Wave motion in a 3-layered, orthotropic isotropic orthotropic composite shell.
9. F. G. YUAN and C. C. HSIEH 1998 *Composite Structures* **42**, 153–167. Three-dimensional wave propagation in composite cylindrical shell.
10. Z. C. XI, L. H. YAM and T. P. LEUNG 1996 *International Journal of Solids and Structures* **33**, 851–863. Semi-analytical study of free vibration of composite shells of revolution based on the Reissner–Mindlin assumption.
11. Z. C. XI, L. H. YAM and T. P. LEUNG 1997 *Composites, Part B* **28B**, 359–375. Free vibration of a laminated composite circular cylindrical shell partially filled with a fluid.
12. Z. C. XI, L. H. YAM and T. P. LEUNG 1997 *The Journal of The Acoustical Society of America* **101**, 909–917. Free vibration of a partially fluid-filled cross-ply laminated composite circular cylindrical shell.
13. Z. C. XI, L. H. YAM and T. P. LEUNG 1999 *International Journal of Mechanical Sciences* **41**, 649–661. Nonlinearly elastic free vibration of a laminated composite shell of revolution.
14. X. HAN, G. R. LIU, Z. C. XI and K. Y. LAM 1999 *International Journal of Solids and Structures* **38**, 3021–3037. Transient waves in a functionally graded cylinder.
15. N. RATTANWANGCHAROEN, A. SHAH and S. K. DATTA 1994 *American Society of Mechanical Engineers, Journal of Applied Mechanics* **61**, 323–329. Reflection of waves at the free edge of a laminated circular cylinder.
16. N. RATTANWANGCHAROEN, W. ZHUANG, A. SHAH and S. K. DATTA 1997 *American Society of Civil Engineers, Journal of Engineering Mechanics* **123**, 1020–1026. Axisymmetric guided waves in jointed laminated cylinders.
17. W. ZHUANG, A. SHAH and S. K. DATTA 1997 *Journal of Pressure Vessel Technology* **119**, 401–406. Axisymmetric guided wave scattering by cracks in welded steel pipes.
18. Z. C. XI, G. R. LIU, K. Y. LAM and H. M. SHANG 2000 *American Society of Mechanical Engineers Journal of Applied Mechanics* **67**, 427–429. Strip element method for analyzing wave scattering by a crack in a laminated composite cylinder.
19. Z. C. XI, G. R. LIU, K. Y. LAM and H. M. SHANG 2000 *Composites Science and Technology* **60**, 1985–1996. Strip element method for analyzing wave scattering by a crack in a fluid-filled laminated composite shell.
20. Z. C. XI, G. R. LIU, K. Y. LAM and H. M. SHANG 2000 *The Journal for Acoustical Society of America* **108**, 175–183. Strip element method for analyzing wave scattering by a crack in an immersed laminated composite cylinder.

21. R. B. NELSON, S. B. DONG and R. D. KALRA 1971 *Journal of Sound and Vibration* **18** 429–444. Vibrations and waves in laminated orthotropic circular cylinders.
22. K. H. HUANG and S. B. DONG 1984 *Journal of Sound and Vibration* **96**, 363–379. Propagating waves and edge vibrations in anisotropic composite cylinders.
23. M. J. BERLINER and R. SOLECKI 1996 *Journal of the Acoustical Society of America* **99**, 1841–1847. Wave propagation in fluid-loaded, transversely isotropic cylinders. Part I: analytical formulation.
24. M. J. BERLINER and R. SOLECKI 1996 *Journal of the Acoustical Society of America* **99**, 1848–1853. Wave propagation in fluid-loaded, transversely isotropic cylinders. Part II: numerical results.
25. Z. C. XI, G. R. LIU, K. Y. LAM and H. M. SHANG 2000 *The Journal for Acoustical Society of America* **108**, 2179–2186. Dispersion and characteristic surfaces of waves in laminated composite circular cylindrical shells.
26. J. R. VINSON and R. L. SIERAKOWSKI 1987 *The Behavior of Structures Composed of Composite Materials*. Dordrecht: Martinus Nijhoff.
27. K. TAKAHASHI and TSU-WEI CHOU 1987 *Journal of Composite Materials* **21**, 396–407. Non-linear deformation and failure behavior of carbon/glass hybrid laminates.
28. G. R. LIU, J. TANI, T. OHYOSHI and K. WATANABE 1991 *Journal of Vibration and Acoustics* **113**, 279–285. Characteristic wave surfaces in anisotropic laminated plates.